Synthesis and Characterization of a Novel Vinyl-2,2′-bipyridine Monomer and Its Homopolymeric/Copolymeric Metal Complexes

Elefterios K. Pefkianakis, Nikolaos P. Tzanetos, and Joannis K. Kallitsis*

Department of Chemistry, University of Patras, 26500 Patras, Greece

Received March 31, 2008. Revised Manuscript Received July 8, 2008

Novel hybrid materials, based on polymeric ruthenium complexes, have been synthesized and characterized. The preparation of a new vinylic tris(bipyridine)ruthenium complex in high yields enabled the synthesis of soluble polymeric materials with high metal loading, using a controlled polymerization technique such as atom transfer radical polymerization. Moreover, combination of this monomeric complex with other monomers, known for their electron or hole transporting properties, led to soluble copolymers of various desired ruthenium loadings. Characterization of the synthesized polymers and copolymers was performed using NMR, SEC, and viscometry. The polymer−metal hybrid materials' optical properties were studied in detail through UV−vis and photoluminescence spectroscopies, showing the [$Ru^{II}(bpy)_3$] complexes' intense optoelectronic characteristics, also in combination with the optical properties of the oxadiazole or carbazole units in the copolymer case.

Introduction

The introduction of metal−ligand bonding into polymers brings novel and potentially useful physical and chemical properties to the final polymeric complexes.[1−5] These properties arise from the combination of both the metal ion (oxidoreductive, optoelectronic, catalytic) and the polymers' characteristics (processability, mechanical strength, thin film formation, etc.). The incorporation of metal binding sites into polymers can be performed either along the main chain[6−11] or as side group functionalities.[12−22] To enable metal complexation, bidentate and tridentate ligands such as 2,2′-bipyridine (bpy) and 2,2′:6′,2″-terpyridine (tpy) are mainly used, as well as some nitrogen-containing heterocycles,[1] through which the introduction of various transition-metal ions such as Fe(II), Cu(II), Os(II), Ir(II), and Ru(II) can be achieved.[1,2,5,6,8,22−28] Among these ions, ruthenium(II) is the most promising for the creation of polymeric metal complexes, since it allows the direct synthesis of both symmetric and nonsymmetric, stable systems.[22−31] Moreover, ruthenium complexes of bipyridine ligands are considered ideal for optoelectronics in comparison to terpyridine ligands, since they present fine absorption properties and higher luminescence and charge transport efficiency.[1,24,25]

In particular, tpy−Ru(II)−tpy complexes have been extensively used as main chain polymeric functionalities for

* To whom correspondence should be addressed. Phone: +30-2610-997121. Fax: +30-2610-997-122. E-mail: j.kallitsis@chemistry.upatras.gr.

(1) Schubert, U. S.; Eschbaumer, C. *Angew. Chem., Int. Ed.* **2002**, *41*, 2829.
(2) Whittell, G. R.; Manners, I. *Adv. Mater.* **2007**, *19*, 3439.
(3) Fustin, C. A.; Guillet, P.; Schubert, U. S.; Gohy, J. F. *Adv. Mater.* **2007**, *19*, 1665.
(4) Williams, K. A.; Boydston, A. J.; Bielawski, C. W. *Chem. Soc. Rev.* **2007**, *36*, 729.
(5) Abruña, H. D.; Denisevich, P.; Umaña, M.; Meyer, T. J.; Murray, R. W. *J. Am. Chem. Soc.* **1981**, *103*, 1.
(6) Heller, M.; Schubert, U. S. *Macromol. Rapid Commun.* **2001**, *22*, 1358.
(7) Guerrero-Sanchez, C.; Lohmeijer, B. G. G.; Meier, M. A. R.; Schubert, U. S. *Macromolecules* **2005**, *38*, 10388.
(8) Chiper, M.; Meier, M. A. R.; Wouters, D.; Hoeppener, S.; Fustin, C.-A.; Gohy, J.-F.; Schubert, U. S. *Macromolecules* **2008**, *41*, 2771.
(9) Knapp, R.; Schott, A.; Rehahn, M. *Macromolecules* **1996**, *29*, 478.
(10) Kelch, S.; Rehahn, M. *Macromolecules* **1997**, *30*, 6185.
(11) Kelch, S.; Rehahn, M. *Macromolecules* **1999**, *32*, 5818.
(12) Jones, W. E., Jr.; Baxter, S. M.; Strouse, G. F.; Meyer, T. J. *J. Am. Chem. Soc.* **1993**, *115*, 7363.
(13) Calzia, K. J.; Tew, G. N. *Macromolecules* **2002**, *35*, 6090.
(14) Aamer, K. A.; De Jeu, W. H.; Tew, G. N. *Macromolecules* **2008**, *41*, 2022.
(15) Serin, J. X.; Andronov, S. A.; Fréchet, J. M. J. *Macromolecules* **2002**, *35*, 5396.
(16) Chen, B.; Sleiman, H. F. *Macromolecules* **2004**, *37*, 5866.
(17) Heller, M.; Schubert, U. S. *Macromol. Rapid Commun.* **2002**, *23*, 411.
(18) Schubert, U. S.; Hofmeier, H. *Macromol. Rapid Commun.* **2002**, *23*, 561.
(19) Dupray, L. M.; Meyer, T. J. *Inorg. Chem.* **1996**, *35*, 6299.
(20) Kajita, T.; Leasure, R. M.; Devenney, M.; Friesen, D.; Meyer, T. J. *Inorg. Chem.* **1998**, *37*, 4782.
(21) Yoshiki, C.; Kazuki, S.; Takeo, S. *Macromolecules* **1993**, *26*, 6320.
(22) Potts, K. T.; Usifert, D. A. *Macromolecules* **1988**, *21*, 1985.
(23) Lamba, J. J. S.; Fraser, C. L. *J. Am. Chem. Soc.* **1997**, *119*, 1801.
(24) Chen, M.; Ghiggino, K. P.; Thang, S. H.; Wilson, G. J. *Angew. Chem., Int. Ed.* **2005**, *44*, 4368.
(25) Potts, K. T.; Usifer, D. A.; Guadalupe, A.; Abruna, H. D. *J. Am. Chem. Soc.* **1987**, *109*, 3961.
(26) Sprintschnik, G.; Sprintschnik, H. W.; Kirsch, P. P.; Whitten, D. G. *J. Am. Chem. Soc.* **1977**, *99*, 4947.
(27) Sullivan, B. P.; Salmon, D. J.; Meyer, T. J. *Inorg. Chem.* **1978**, *17*, 3334.
(28) Aamer, K. A.; Tew, G. N. *Macromolecules* **2007**, *40*, 2737.
(29) Johnson, R. M.; Corbin, P. S.; Ng, C.; Fraser, C. L. *Macromolecules* **2000**, *33*, 7404.
(30) Fraser, C. L.; Smith, A. P. *J. Polym. Sci., Part A: Polym. Chem.* **2000**, *38*, 4704.
(31) Wu, X.; Collins, J. E.; McAlvin, J. E.; Cutts, R. W.; Fraser, C. L. *Macromolecules* **2001**, *34*, 2812.
(32) Aamer, K. A.; Tew, G. N. *J. Polym. Sci., Part A: Polym. Chem.* **2007**, *45*, 1109.
(33) Tzanetos, N. P.; Kallitsis, J. K. *J. Polym. Sci., Part A: Polym. Chem.* **2005**, *43*, 1049.
(34) Tzanetos, N. P.; Andreopoulou, A. K.; Kallitsis, J. K. *J. Polym. Sci., Part A: Polym. Chem.* **2005**, *43*, 4838.
(35) Andreopoulou, A. K.; Kallitsis, J. K. *Eur. J. Org. Chem.* **2005**, *2005*, 4448.
(36) Chen, M.; Ghiggino, K. P.; Launikonis, A.; Mau, A. W. H.; Rizzardo, E.; Sasse, W. H. F.; Thang, S. H.; Wilson, G. J. *J. Mater. Chem.* **2003**, *13*, 2696.

10.1021/cm800911y CCC: $40.75
Published on Web 09/10/2008

the creation of coordination polymers. Terpyridine end-functionalized oligomers or well-defined polymeric chains that are afterward linked together through metal−ligand coordination bonding, forming supramolecular block copolymers, have mainly been reported by the group of Schubert.[6−8,17,18] In addition, preformed block copolymers produced by controlled polymerization techniques that are being postmodified with side tpy−Ru(II)−tpy complexes have been synthesized and extensively studied by Tew's group.[14,28,32] Initially, low metal loadings were reported, to ensure the solubility of the final hybrid material. This methodology was later extended to copolymers with higher metal loadings, using alkyl-tail-functionalized terpyridines, which further increased their solubility and self-organizational ability.[14,28] In another approach, our group reported on the synthesis of soluble homopolymers bearing side chain tpy−Ru(II)−tpy moieties. Atom transfer radical polymerization (ATRP) of a tpy-containing vinylic monomer and the subsequent complexation, using alkoxy-decorated tpy−Ru(II) monocomplexes, resulted in highly metal loaded soluble homopolymers.[33,34] All the above-mentioned approaches are mainly based on tpy ligands, and the solubility was assured either by low metal loadings[13,14] or by the use of aliphatic units either as spacers or as decorating tails.[35]

As far as the ruthenium tris(bipyridine), $[Ru^{II}(bpy)_3]^{2+}$, coordination polymeric complexes are concerned, various attempts have also been described. Polymers and copolymers with main or side chain $[Ru^{II}(bpy)_3]^{2+}$ units and their possible applications in optoelectronics have been reported.[1−3,12,17,20] Rehahn's group was the first to report on well-defined, high molecular weight, soluble coordination polymers of $[Ru^{II}(bpy)_3]^{2+}$ complexes and their UV−vis and viscosity properties.[9−11] The polymerization of $[Ru^{II}(bpy)_3]^{2+}$ complexes using reductive polymerization techniques was first described by Murray's group,[5] while copolymers where the ruthenium complexes were attached to a preformed polymeric backbone through a nucleophilic displacement were produced by the group of Meyer.[12,19,20,26] Later, Fraser's group used $[Ru^{II}(bpy)_3]^{2+}$ cores as initiators for ATRP (*divergent synthesis*) or as coupling agents of ATRP-prepared polymers (*convergent synthesis*) to produce well-defined linear and star-shaped polymers (e.g., polystyrene, poly(methyl methacrylate)),[23,29−31] a procedure also performed by Ghiggino utilizing RAFT polymerization techniques.[24,36]

However, up to now, besides the free radical polymerization (FRP)[15] and ring opening metathesis polymerization (ROMP)[16] of vinyl $[Ru^{II}(bpy)_3]^{2+}$ complexes, there have been no attempts to apply other controlled polymerization techniques, though control over molecular architecture is one of the most important scopes in this field of polymer science, since it determines to a great extent the properties of the final supramolecular material.[1−4] Especially for optoelectronic applications such as light-emitting diodes (LEDs) and photovoltaics (PVs), the charge transport and the electron donor/acceptor phase separation and interactions are the major issues determining their efficiency. Well-defined polymeric metal complexes for such applications can be prepared through controlled polymerizations of precursor polymeric chains and their complexation thereafter[6,14,16,19] or polymerization of preformed monomeric complexes.[17]

Among the different controlled polymerization techniques, the ATRP methodology[37−40] is tolerant of a number of functional groups, located on either the initiator or the vinylic monomers used, thus being a useful tool in providing homopolymers or copolymers of well-defined molecular characteristics. However, the ATRP methodology for producing homopolymers of monomeric complexes having $[Ru^{II}(bpy)_3]^{2+}$ moieties has not been presented up to now.

This work focuses on the synthesis and characterization of a vinyl-2,2′-bipyridine monomer and its resulting metal complex with Ru(II) ions and is the first report on atom transfer radical homopolymerization of such complexes using functional initiators.[33,34,41] The use of the initiators reported here will help in the further functionalization of these polymers, allowing their implementation in other reactions. As an example, the synthesized homopolymers could be introduced in polycondensation reactions or even be used in hybrid solar cells as ruthenium-containing polymeric dyes. Also FRP was applied to this new $[Ru^{II}(bpy)_3]^{2+}$ complex in combination with electron or hole transporting monomers such as oxadiazoles and carbazoles, respectively. All polymers produced were fully characterized and evaluated with respect to their structural characteristics and optical properties.

Experimental Section

Materials. Dichlorobis(2,2′-bipyridine)ruthenium(II) [*cis*-$(bpy)_2RuCl_2\cdot 2H_2O$],[26] tetrakis(triphenylphosphine)palladium $[Pd(PPh_3)_4]$,[42] 4-styrylboronic acid,[43] and 2-{4-[(4-vinylphenyl)methoxy]phenyl}-5-phenyl-1,3,4-oxadiazole[44] were produced according to the literature. 2,2′-Azobis(2-methylpropionitrile) (AIBN) was recrystallized from MeOH, diethyl ether (DEE) was distilled from Na wire, and tetrahydrofuran (THF) was distilled from Na wire in the presence of benzophenone. All other reagents and solvents were purchased by Aldrich and used as received. All reactions and polymerizations were carried out under an inert argon atmosphere.

Instrumentation. The structures of the synthesized monomers, polymers, and copolymers were clarified by high-resolution ^1H NMR and ^{13}C NMR spectroscopy with Bruker Avance DPX 400 and 100 MHz spectrometers, respectively. The samples were dissolved in deuterated chloroform ($CDCl_3$) or deuterated dimethyl sulfoxide (DMSO-d_6), using tetramethylsilane (TMS) as the internal standard.

In the case of copolymers with low metal complex content, molecular weights (M_n, M_w, PDI) were determined by gel permeation chromatography using a Polymer Laboratory chromatograph (Ultrastyragel columns with 500 and 10^4 Å pore sizes) calibrated with polystyrene standards using $CHCl_3$ (filtered through a 0.5 μm Millipore filter, analytical grade) as the eluent at a flow rate of 1 $mL\cdot min^{-1}$ at room temperature (rt) and equipped with a UV detector (254nm) along with a "Schodex RI-101" refractive index detector.

(37) Wang, J. S.; Matyjaszewski, K. *Macromolecules* **1995**, *28*, 7901.
(38) Matyjaszewski, K. *Chem.—Eur. J.* **1999**, *5*, 3095.
(39) Matyjaszewski, K.; Xia, J. *Chem. Rev.* **2001**, *101*, 2921.
(40) Kamigaito, M.; Ando, T.; Sawamoto, M. *Chem. Rev.* **2001**, *101*, 3689.
(41) Deimede, V.; Kallitsis, J. K. *Chem.—Eur. J.* **2002**, *35*, 1487.
(42) Coulson, D. R. *Inorg. Synth.* **1972**, *13*, 121.
(43) Dondoni, A.; Ghiglione, C.; Marra, A.; Scoponi, M. *J. Org. Chem.* **1998**, *63*, 9535.
(44) Tzanetos, N. P.; Kallitsis, J. K. *Chem. Mater.* **2004**, *16*, 2648.

The UV spectra were recorded on a Hitachi spectrophotometer, model U-1800. Photoluminescence spectra were obtained using a Perkin-Elmer LS45 luminescence spectrometer by excitation of the sample at the absorption maxima of the UV−vis spectra. All spectroscopic measurements were performed in quartz glass cuvettes (1 cm) at concentrations of $10^{-5}-10^{-6}$ M with respect to the repeating units. Viscosity measurements were carried out in DMF solutions with an Ostwald-type viscometer at 30 °C in a Scott Gerate AVS 310 apparatus.

Monomer Synthesis. *2-(Tributylstannyl)pyridine (**a**).* To a degassed three-necked round-bottom flask equipped with a reflux condenser, an addition funnel, and a magnetic stirrer under an argon atmosphere was added 4.25 g (2.56 mL, 26.90 mmol) of 2-bromopyridine. Through the addition funnel 50 mL of distilled DEE was added dropwise. Then the system was cooled to −80 °C followed by the dropwise addition of *n*-BuLi (1.6 M solution in *n*-hexane, 21 mL, 33.60 mmol). The reaction mixture was kept at the same low temperature for 3 h. Afterward, 9.12 mL (33.60 mmol) of tributylzinc chloride was added through the funnel, and the reaction mixture was stirred at −80 °C for another 3 h and then at rt for 12 h. Then all solvents were evaporated under vacuum, and 60 mL of distilled DEE was added. The mixture was filtered to remove any solid impurities, and the filtrate was evaporated under reduced pressure. The resulting 2-(tributylstannyl)pyridine was used in the following reaction without any further treatment. Yield: 8.41 g (85%).

*5-Bromo-2,2′-bipyridine (**b**).* To a degassed round-bottom flask equipped with a reflux condenser and a magnetic stirrer under an argon atmosphere were added 6.77 g (28.60 mmol) of 2,5-dibromopyridine and 0.66 g (0.57 mmol) of $Pd(PPh_3)_4$. The system was degassed again, and the solid from the previous reaction, 8.41 g (22.90 mmol) of 2-(tributylstannyl)pyridine, was added dissolved in 50 mL of dry xylene under an argon atmosphere. The reaction mixture was then heated at 120 °C for 14 h. After the reaction mixture was cooled to rt, 60 mL of aqueous NaOH (2 M) was added. The mixture was extracted with toluene and dried over $MgSO_4$. The solvent was evaporated under vacuum, and the crude solid product was purified via column chromatography (silica gel, 230−400 mesh, ASTM) using *n*-hexane/ethyl acetate (5:1) as the eluent. The desired product was obtained as a white crystalline powder which was dried at 45 °C under vacuum. Yield: 3.51 g (65%). ^{1}H NMR ($CDCl_3$): 7.33 (ddd, 1H), 7.82 (td, 1H), 7.94 (dd, 1H), 8.32 (d, 1H), 8.37 (d, 1H) 8.67 (dt, 1H), 8.72 (d, 1H) ppm. ^{13}C NMR ($CDCl_3$): 120.92, 121.09, 122.29, 123.96, 136.97, 139.45, 149.21, 150.15, 154.58, 155.13 ppm.

*5-(*p*-Vinylphenyl)-2,2′-bipyridine (**c**).* To a degassed three-necked round-bottom flask equipped with a reflux condenser, an addition funnel, and a magnetic stirrer under an argon atmosphere were added 0.80 g (3.40 mmol) of 5-bromo-2,2′-bipyridine, 0.75 g (5.10 mmol) of 4-styrylboronic acid, and 0.15 g (0.13 mmol) of $Pd(PPh_3)_4$. The system was degassed again, and 70 mL of distilled THF and 6.37 mL of K_2CO_3 (2 M) degassed aqueous solution were added. The reaction mixture was refluxed for 48 h. After being cooled to rt, the mixture was extracted using toluene and dried over $MgSO_4$. The solvent was removed under vacuum, the resulting yellow solid was stirred for 2 h in *n*-hexane and filtered to remove any impurities, and the filtrate was evaporated. A white powder was obtained after the residue was dried under reduced pressure at 30 °C for 24 h. Yield: 0.75 g (85%). Purity by ^{1}H NMR: 90%. The product was further purified via column chromatography (silica gel, 230−400 mesh, ASTM) using dichloromethane, which elutes the impurities, and then dichloromethane/MeOH (20:1), which elutes the desired clean product. The yield by chromatography was 85%, and the purity of the product was estimated as 100% by ^{1}H NMR spectroscopy. ^{1}H NMR ($CDCl_3$): 5.32 (d, 1H), 5.83 (d, 1H), 6.78 (q, 1H), 7.33 (ddd, 1H), 7.53 (d, 2H), 7.63 (d, 2H), 7.84 (td, 1H), 8.03 (dd, 1H), 8.45 (q, 2H), 8.71 (d, 1H) 8.93 (d, 1H) ppm.

Scheme 1. Synthetic Route toward [5-(*p*-Vinylphenyl)-2,2′-bipyridine]bis(2,2′-bipyridine)ruthenium(II), $[Ru(vbpy)(bpy)_2](PF_6)_2$ (d)

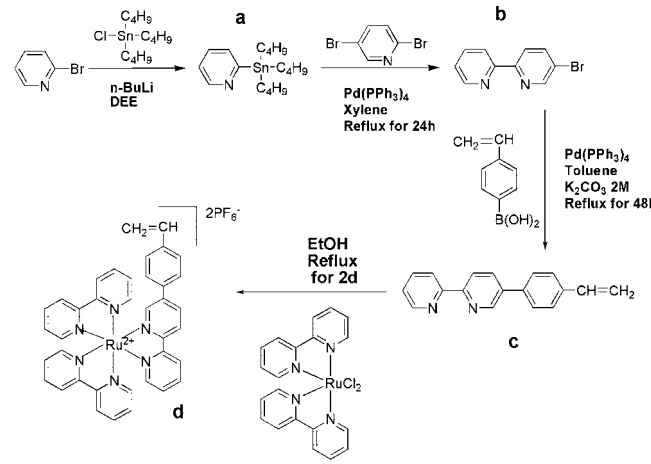

*[5-(*p*-Vinylphenyl)-2,2′-bipyridine]bis(2,2′-bipyridine)ruthenium(II), $[Ru^{II}(vbpy)(bpy)_2](PF_6)_2$ (**d**).* To a degassed round-bottom flask equipped with a reflux condenser and a magnetic stirrer under an argon atmosphere were added 0.12 g (0.47 mmol) of **c**, 0.16 g (0.31 mmol) of $[cis\text{-}(bpy)_2RuCl_2\cdot 2H_2O]$,[26] and 30 mL of absolute EtOH. The reaction mixture was degassed once again and refluxed for 72 h. The resulting red-colored mixture was cooled to rt, and the solvent was evaporated under reduced pressure, affording an orange powder. Afterward 40 mL of deionized water was added, and the mixture was stirred for 0.5 h, followed by filtration to remove solid impurities. To the filtrate was added 20 mL of an aqueous solution of NH_4PF_6, which caused the formation of orange crystals to precipitate spontaneously. The crystals formed were filtered and washed with deionized water to remove the excess NH_4PF_6 and consecutively with DEE. Drying under vacuum at 45 °C for 24 h afforded the final product. Yield: 0.270 g (87%). ^{1}H NMR (DMSO-d_6): 5.33 (d, 1H), 5.94 (d, 1H), 6.75 (q, 1H), 7.46 (d, 2H), 7.51−7.58 (m, 7H), 7.71−7.78 (m, 4H), 7.86 (d, 1H), 7.91 (d, 1H), 8.14−8.23 (m, 5H), 8.51 (dt, 1H), 8.79−.92 (m, 6H) ppm. ^{13}C NMR (DMSO-d_6): 116.57, 124.92, 124.97, 125.05, 125.14, 127.53, 127.61, 128.27, 128.32, 128.46, 134.03, 135.82, 136.12, 138.43, 138.76, 138.88, 148.39, 151.70, 152.16, 152.30, 155.71, 156.82, 156.91, 157.02, 157.12, 157.21 ppm.

Polymerizations. *Atom Transfer Radical Polymerization using Functional Initiators.* A round-bottom flask equipped with a rubber septum, a magnetic stirrer, and a gas inlet/outlet was flamed under vacuum. Initiator 5-[[4-(bromomethyl)benzyl]oxy]benzene-1,3-dioic acid (**Ia**),[33,41] 5.72 mg (0.02 mmol), or the distyrylanthrcene derivative **II**,[34] 11.94 mg (0.02 mmol) (shown in Schemes 2 and 3), was added to the flask which contained CuBr, 5.75 mg (0.04 mmol), and 8.4 μL (0.04 mmol) of *N*,*N*,*N*′,*N*″,*N*″-pentamethyldiethylenetriamine (PMDETA). The system was degassed three times and flushed with argon. The solvent dimethyl formamide (DMF) and 385 mg (0.4 mmol) of monomer **d** were added to the flask, and the mixture was immediately degassed and flushed with argon three times. The reaction mixture was then immersed in an oil bath and heated at 110 °C for 24 h. After the reaction mixture was cooled to room temperature, 2 mL of DMF was added to dissolve the polymer. The suspension was filtered from silica gel to remove most of the catalyst. The resulting polymer was precipitated as a dark-orange crystalline-like powder in 20-fold excess by volume of methanol. Filtration and excessive washing

Scheme 2. Atom Transfer Radical Polymerization of Monomer d and Its Kinetic Study (I/M versus Time)

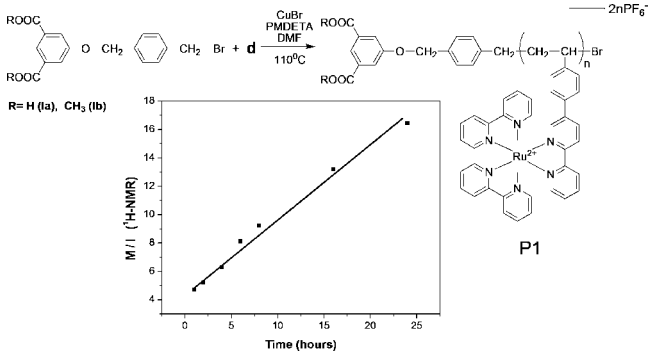

Table 1. Characterization of Polymers P1 and P2

polymer	feed ratio, initiator/ monomer	no. of monomers attached	M_n estimation by ^{1}H NMR	η_{red}[a] at $C = 0.5$ mg/mL
P1a	1/05	7	~7100	
P1b	1/10	9	~9000	
P1c	1/10	10	~10000	
P1d	1/10	13	~12900	41.77
P1e	1/15	16	~16300	
P2a	1/06			11.19
P2b	1/10			21.92
P2c	1/20			51.80

[a] In DMF at 30 °C.

with MeOH and DEE removed any remaining impurities. The final polymeric material was dried under vacuum at 45 °C overnight. The results for the different prepared polymers are summarized in Table 1. ^{1}H NMR (DMSO-d_6) for polymers **P1**: 3.90 (s), 4.55(s), 5.30 (s), 7.55 (br), 7.74 (br), 7.95 (br), 8.17 (br), 8.81 (br) ppm. ^{1}H NMR (DMSO-d_6) for polymers **P2**: 6.87 (br), 7.54 (br), 7.74 (br), 7.95 (br), 8.17 (br), 8.81 (br) ppm.

Free Radical Polymerization: General Procedure. To a degassed round-bottom flask equipped with a magnetic stirrer and a gas inlet/outlet were added the desired amounts of monomer **d** and of oxadiazole monomer (2-{4-[(4-vinylphenyl)methoxy]phenyl}-5-phenyl-1,3,4-oxadiazole, OXD) or carbazole monomer (9-vinylcarbazole, CARB), along with the respective amounts of AIBN. Then 3 mL of DMF was added, and the system was flushed with argon and immersed into an oil bath at 110 °C for 4 days. Then the reaction mixture was allowed to cool at room temperature and was precipitated in 20-fold excess by volume of the solvent required in each case.

For copolymers **P3**, the synthesis of **P3iv** (feed ratio 15/85 OXD/monomer **d**) is presented as an example: A 16 mg (0.042 mmol) portion of the OXD monomer and 240 mg (0.250 mmol) of monomer **d** were added to the flask along with 1.23 mg (0.003 mmol) of AIBN and 3 mL of DMF. The reaction mixture was immersed into an oil bath at 110 °C for 4 days and then precipitated in 60 mL of methanol. Depending on the molar ratio of the copolymers, they were precipitated in methanol or methanol/ethyl acetate or methanol/water mixtures as the percentage of the oxadiazole unit increased, respectively. After filtration the polymers were further washed with methanol and ethyl acetate, to remove any excess of monomers, and consecutively with DEE and dried under vacuum at 45 °C overnight. The copolymers obtained were further purified by reprecipitation from $CHCl_3$ or acetonitrile in DEE. The results are summarized in Table 2. ^{1}H NMR (DMSO-d_6) for copolymers **P3**: 1.5−2.4 (br, 3H of **d** plus 3H of OXD), 4.9 (br, 2H of OXD), 6.2−8.3 (br, 20H of **d** plus 13H of OXD), 8.4−8.9 (br, 7H of **d**) ppm.

Table 2. Molecular Characteristics of Copolymers P3

copolymer, OXD/Ru	composition, ^{1}H NMR	M_n[a]	M_w[a]	PDI[a]
P3i, 95/5	96/04	3100	6900	2.20
P3ii, 90/10	94/06	4100	5100	1.25
P3iii, 85/15	86/14	2700	3200	1.20
P3iv, 75/25	80/20			
P3v, 50/50	60/40			
P3vi, 15/85	22/78			
P3vii, 10/90	13/87			

[a] M_n, M_w, and PDI (M_w/M_n) from GPC measurements using $CHCl_3$ as the eluent and polystyrene standards.

Table 3. Molecular Characteristics of Copolymers P4

copolymer, CARB/Ru	composition,^{1}H NMR	M_n[a]	M_w[a]	PDI[a]
P4i, 95/5	90/10	17400	22300	1.30
P4ii, 85/15	73/27	14500	19300	1.35
P4iii, 75/25	67/33	29100	47600	1.65
P4iv, 50/50	54/46			
P4v, 25/75	33/67			
P4vi, 15/85	23/77			
P4vii, 10/90	14/86			

[a] M_n, M_w, and PDI (M_w/M_n) from GPC measurements using $CHCl_3$ as the eluent and polystyrene standards.

For the **P4** copolymers an example for the synthesis of **P4iv** (for a feed ratio of 50/50 CARB/monomer **d**) is presented: A 29 mg (0.015 mmol) portion of the CARB monomer and 144 mg (0.015 mmol) of monomer **d** were added to the flask along with 1.23 mg (0.003 mmol) of AIBN. The system was degassed and flushed with argon again. Then 3 mL of DMF was added, and the reaction mixture was immersed in an oil bath at 110 °C for 4 days. The copolymers were obtained by precipitation in 20-fold excess by volume of methanol and were further purified by reprecipitation from $CHCl_3$ or acetonitrile in DEE. The results are summarized in Table 3. ^{1}H NMR (DMSO-d_6) for copolymers **P4**: 1.5−2.4 (br, 3H of **d** plus 3H of CARB), 5.7−8.3 (br, 20H of **d** plus 13H of CARB), 8.6−8.9 (br, 7H of **d**) ppm.

Results and Discussion

The synthesis of the vinylic ruthenium complex **d** (Scheme 1) was based on the novel vinylphenyl-2,2′-bipyridine monomer **c**, produced from the brominated bipyridine derivative **b**.[45−54] The synthesis of monobromobipyridine derivatives in the past, was mainly based on bromination under harsh reaction conditions,[47] resulting in low yields. Recently the use of stannyl reagents has provided another way to produce these derivatives in better yields and under milder conditions.[45] In this work, for producing derivative **b**, we employed a procedure slightly modified with respect to the use of (trimethylstannyl)pyridine,[45] by utilizing 2-(tributylstannyl)pyridine (**a**) under the same mild condi-

(45) Schwab, P. F. H.; Fleischer, F.; Michl, J. *J. Org. Chem.* **2002**, *67*, 443.
(46) Smith, A. P.; Corbin, P. S.; Fraser, C. L. *Tetrahedron Lett.* **2000**, *41*, 2787.
(47) Romero, F. M.; Ziessel, R. *Tetrahedron Lett.* **1995**, *36*, 6471.
(48) Zoltewicz, J. A.; Cruskie, M. P., Jr *Tetrahedron* **1995**, *51*, 11393.
(49) El-ghayoury, A.; Ziessel, R. *J. Org. Chem.* **2000**, *65*, 7757.
(50) Malm, J.; Bjoerk, P.; Gronowitz, S.; Hörnfeldt, A. B. *Tetrahedron Lett.* **1992**, *33*, 2199.
(51) Peters, D.; Hörnfeldt, A. B.; Gronowitz, S. *J. Heterocycl. Chem.* **1990**, *27*, 2165.
(52) Miyaura, N.; Suginome, H.; Suzuki, A. *Tetrahedron* **1983**, *39*, 3271.
(53) Miyaura, N.; Ishiyama, T.; Ishikawa, M.; Suzuki, A. *Tetrahedron Lett.* **1986**, *27*, 6369.
(54) Savage, S. A.; Smith, A. P.; Fraser, C. L. *J. Org. Chem.* **1998**, *63*, 10048.

Scheme 3. Molecular Representation of Polymers P1 and P2[a]

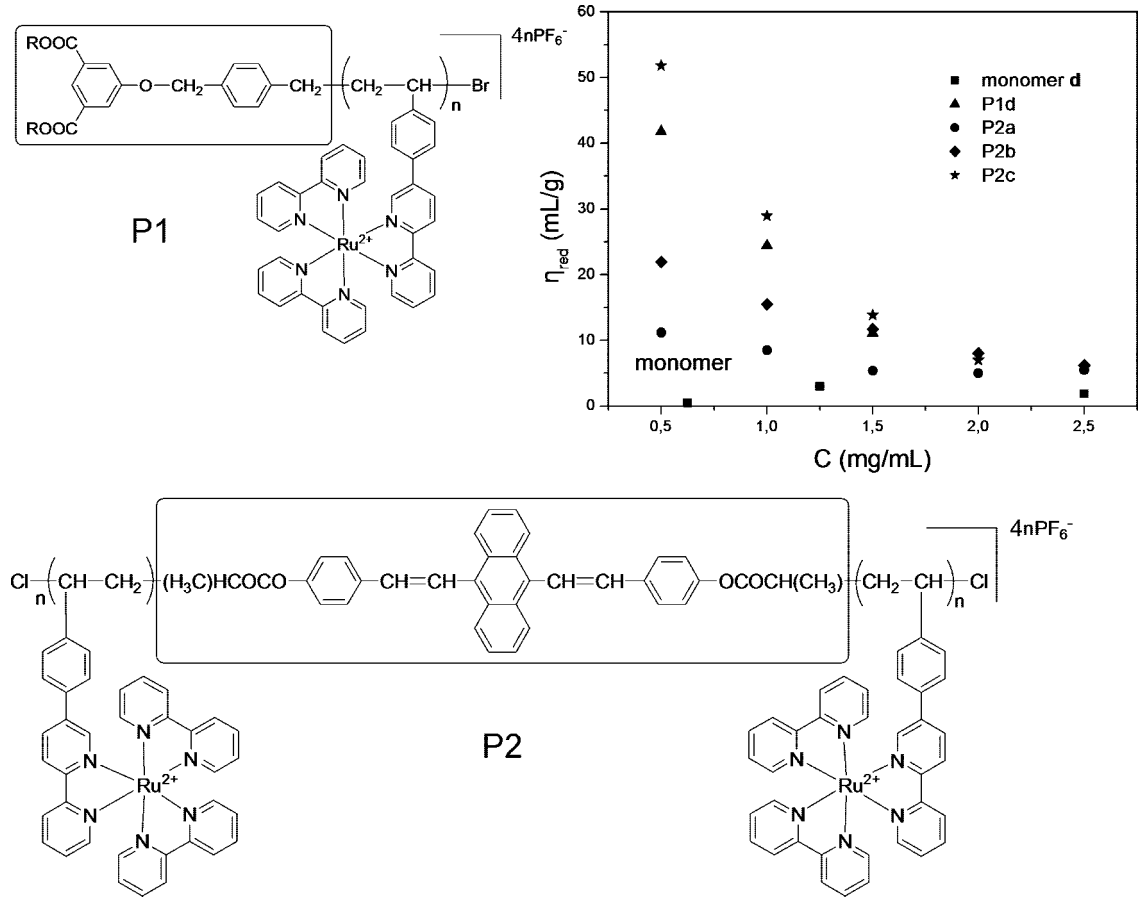

[a] The frames show the initiators used. Inset: viscosity measurements for **P1d** (▲), **P2a** (●), **P2b** (◆), **P2c** (★), and monomer **d** (■) in DMF at 30 °C.

tions. Taking advantage of the Stille coupling reaction[45,48,53] between compound **a** and 2,5-dibromopyridine, combined with the different reactivities between the bromine atoms, we obtained higher yields for the desired monobromobipyridine **b**. As a consequence, the vinylbipyridine monomer **c** was produced via a Suzuki coupling reaction[45,52,53] between compound **b** and 4-styrylboronic acid.[43] Finally the vinyl complex monomer **d** was produced after a complexation reaction of compound **c** with dichlorobis(2,2′-bipyridine)ruthenium(II),[26] followed by counterion exchange from a saturated aqueous solution of NH_4PF_6. Clarification of its chemical structure was performed by ^1H and ^{13}C NMR spectroscopy (Figure 1; see also the Experimental Section).

Homopolymers of monomer **d** were synthesized via ATRP using functional or chromophoric initiators (**Ia**, dicarboxylic acid, and **Ib**, dicarboxylic acid methyl ester,[33,41] or the distyrylanthracene **II** derivative,[34] respectively, Schemes 2 and 3). On the other hand, free radical copolymerization of monomer **d** with oxadiazole or carbazole monomers resulted in electron/hole transporting polymeric architectures (Figures 3 and 4).

In particular, using different initiators (monofunctional **Ia** and **Ib** and bifunctional **II**) and the $[Ru(vbpy)(bpy)_2](PF_6)_2$ unit (**d**), we performed controlled ATR polymerizations that produced well-defined, easily soluble homopolymeric (**P1**) and polymeric triblock (**P2**) complexes. Monomer **d** and the synthesized polymers were characterized via ^1H NMR,

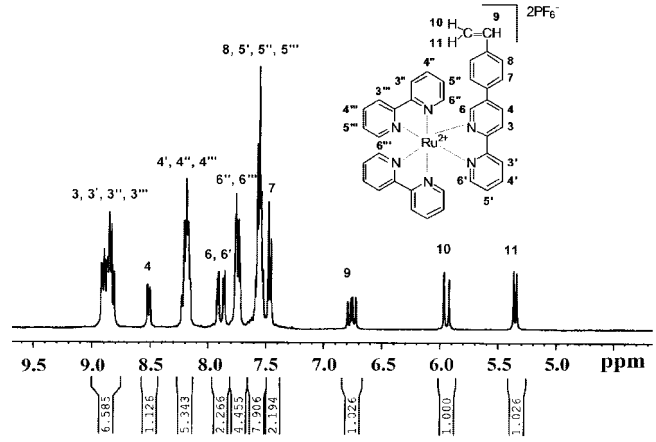

Figure 1. ^1H NMR spectra of monomer **d** in DMSO-d_6.

UV−vis, and photoluminescence (PL) spectroscopy. These polymeric complexes exhibit excellent solubility properties in polar nonprotic solvents, such as acetone, CH_3CN, DMF, and DMSO. The functional initiators of **P1** homopolymers, having dicarboxylic acid methyl ester or dicarboxylic acid functionalities, allow the design and synthesis of more complex architectures (e.g., comb- or starlike structures) since they can be utilized in subsequent reactions such as polycondensations or they can even be directly applied in hybrid solar cells. Additionally all copolymers produced by the FRP

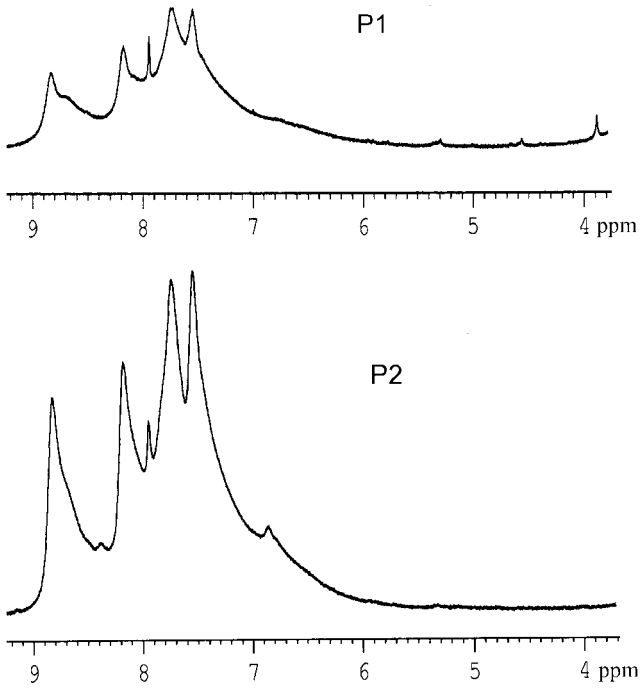

Figure 2. ^{1}H NMR spectrum of polymers **P1** and **P2** in DMSO-d_6.

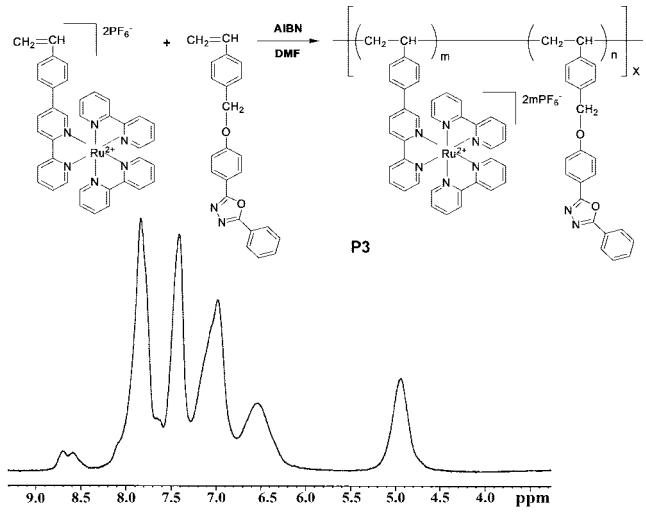

Figure 3. Synthesis of copolymers **P3** and ^{1}H NMR spectrum of **P3iv** in DMSO-d_6.

technique exhibit the same solubility properties and were similarly characterized.

On the basis of the ^{1}H NMR spectra of polymers **P1** and **P2**, shown in Figure 2, the successful ATR polymerization is proved, since the olefins' peaks at 5.33, 5.94, and 6.75 ppm of the bpy monomer are not present. The case of thermal polymerization is also excluded, since the protons of the initiators are evident. Thus, in the case of **P1**, as shown in Figure 2, the peaks at 3.90, 4.55, and 5.30 ppm attributed to the methyl and methylene protons of the initiator **Ia** can be used to calculate the polymers' M_n. The results of these calculations are presented in Table 1, showing the close agreement between the feed ratio of initiator to monomer and the calculated M_n. This is another piece of evidence of a successful ATR polymerization and not just a conventional radical or thermal polymerization. Moreover, to prove the

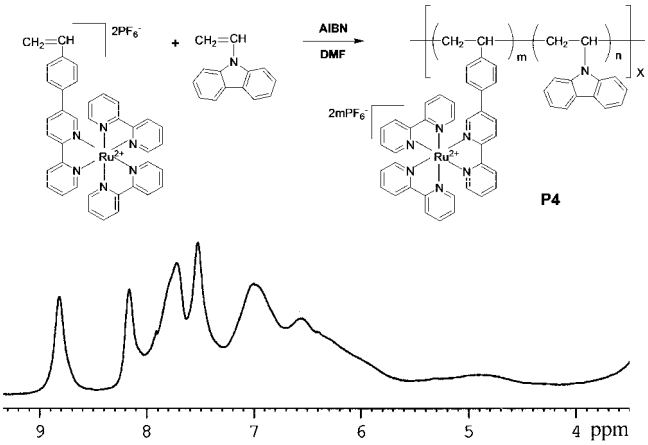

Figure 4. Synthesis of copolymers **P4** and ^{1}H NMR spectrum of **P4ii** in DMSO-d_6.

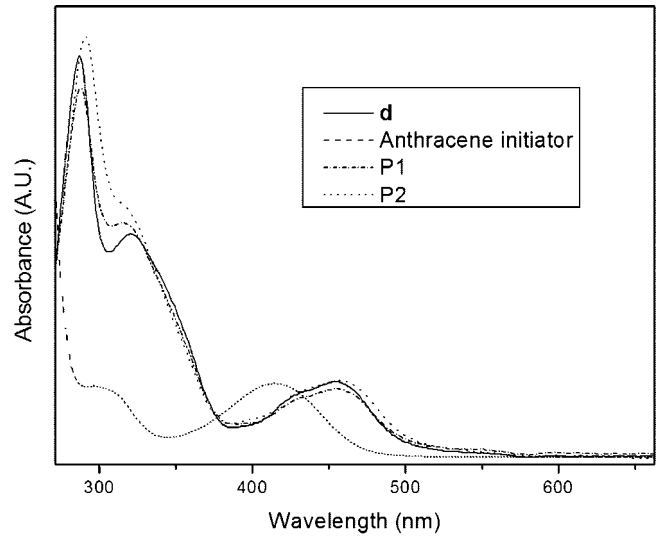

Figure 5. UV−vis absorption spectra of monomer **d**, polymers **P1** and **P2**, and the anthracene initiator **II** used in **P2** in DMF.

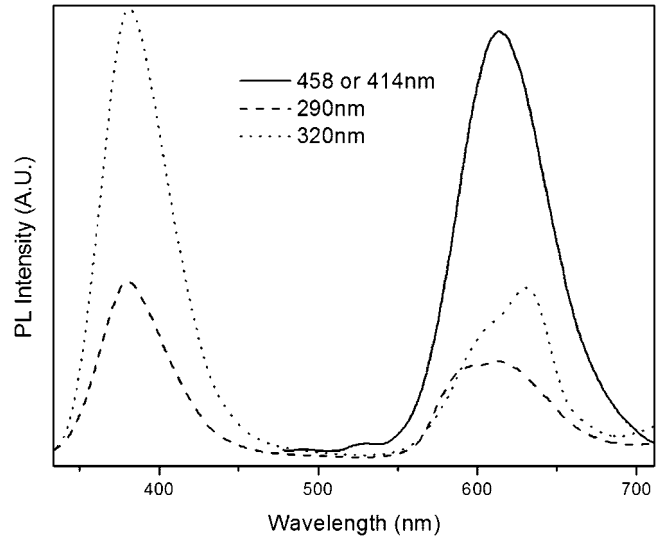

Figure 6. PL spectra of polymer **P2** after excitation at λ = 290, 320, and 458 nm in DMF.

controlled character of these polymerizations, we performed kinetic studies that were carried out analogously to the general polymerization procedure. We selected the monomer

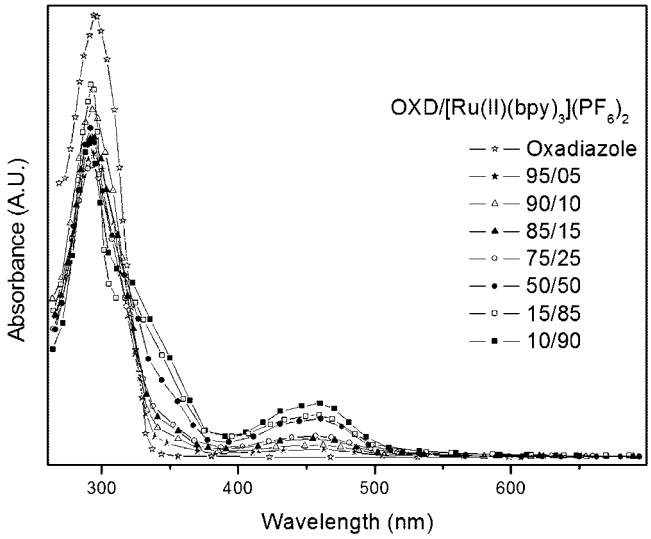

Figure 7. UV−vis absorption spectra of copolymers **P3** and of the oxadiazole monomer in DMF.

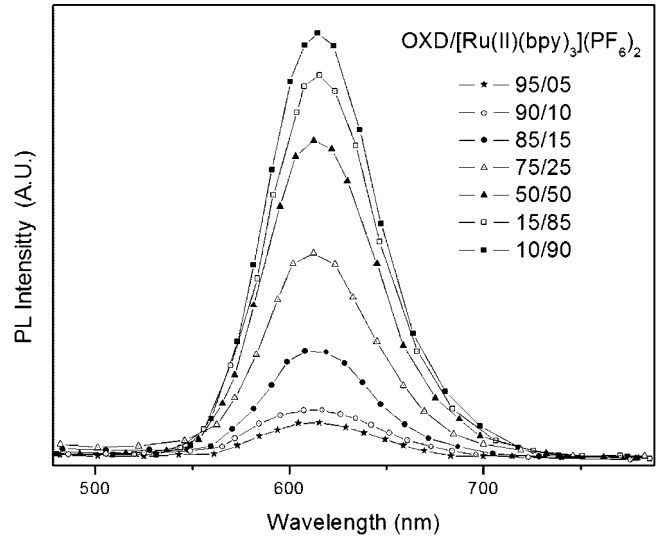

Figure 9. PL spectra of copolymers **P3** after excitation at $\lambda = 458$ nm in DMF.

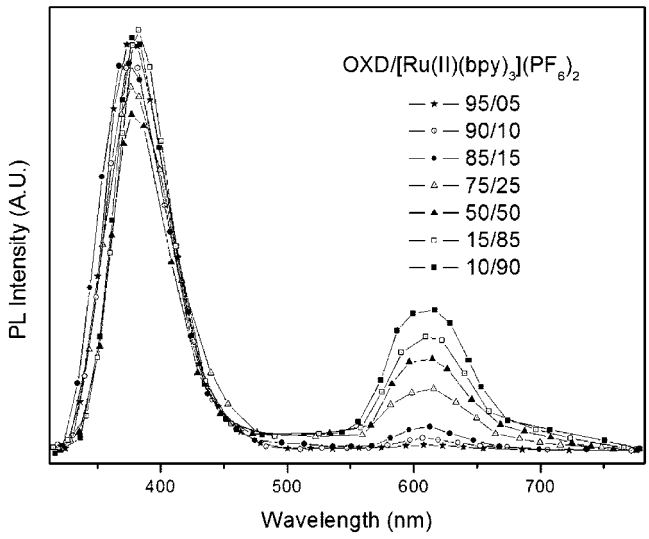

Figure 8. PL spectra of copolymers **P3** after excitation at $\lambda = 290$ nm in DMF.

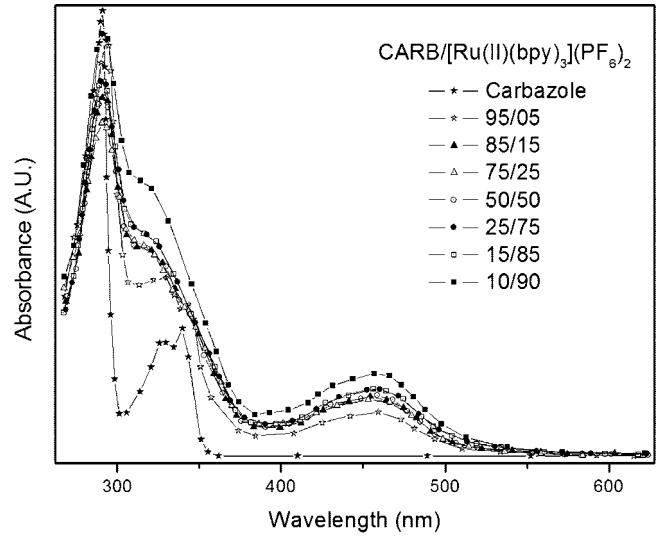

Figure 10. UV−vis absorption spectra of copolymers **P4** and of the carbazole monomer in DMF.

d/initiator **Ia**/CuBr/PMDETA (15/1/2/2) system for a kinetic study. During the reaction time, seven samples of 0.30 mL were withdrawn, and each one was precipitated in 20 mL of deionized water. This way, the catalytic complex of copper/PMDETA was diluted; the samples were centrifuged and washed again with water three times. Finally the same procedure was repeated three times with diethyl ether to remove any trace of unreacted initiator. Thus, the ^{1}H NMR end group analysis technique was used to estimate the true M_n values of our polymers during the polymerization. The M_n values were determined by ^{1}H NMR spectroscopy from the signal at $\delta = 3.9$ ppm corresponding to the methyl protons of the **Ia** initiator used (6 protons) and the whole region from 7.3 to 8.9 ppm corresponding to the aromatic protons of both the monomer (27 protons) and the polymer (27 protons). A representative ^{1}H NMR spectrum of the α-dicarboxylic acid methyl ester **Ib** initiated polymer **P1** for the kinetic study, with the assignment of all peaks, is depicted in the Supporting Information (Figure S1). The plot of initiator monomer (M)/(I) versus time is linear, indicating that the number of growing radicals remained constant throughout the polymerization (Scheme 2). Concerning polymer **P2**, there are no selective peaks for both the initiator **II** and the polymer to obtain the M_n value through the ^{1}H NMR technique in this case.

For the copolymers of the ruthenium complex with oxadiazole units (**P3**), the composition ratio could be calculated from the ^{1}H NMR spectra, since selective peaks can be observed. Composition calculations were based on the ^{1}H NMR peak at 8.4−8.9 ppm, attributed to six of the bpy aromatic protons of the $[Ru(vbpy)(bpy)_2]^{2+}$ unit, and the peak at 5.0 ppm, attributed to the methylene protons in the α-position to the oxygen atom of the side oxadiazole unit (Figure 3).

In the case of copolymers of the ruthenium complex with carbazole units (**P4**), the composition ratio could once again be estimated by the ^{1}H NMR spectra, though roughly, due to the low discrimination of the respective monomers and

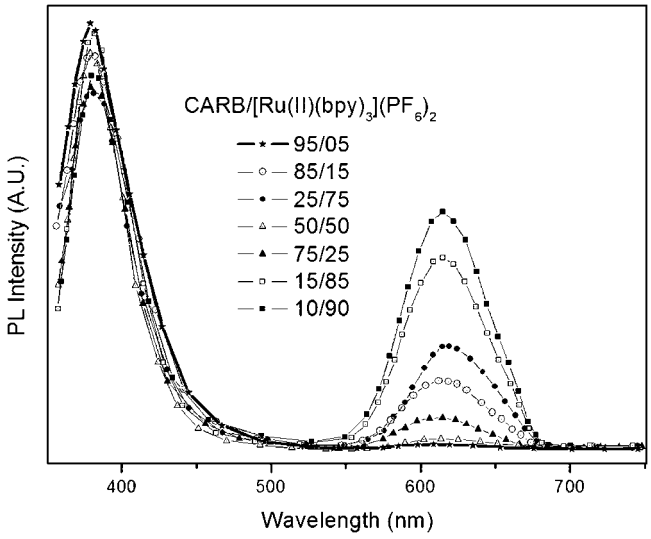

Figure 11. CARB/[Ru(II)(bpy)$_3$](PF$_6$)$_2$: 95/05 = ★, 85/15 = △, 75/25 = ▲, 50/50 = ○, 25/75 = ●, 15/85 = □, 10/90 = ■.

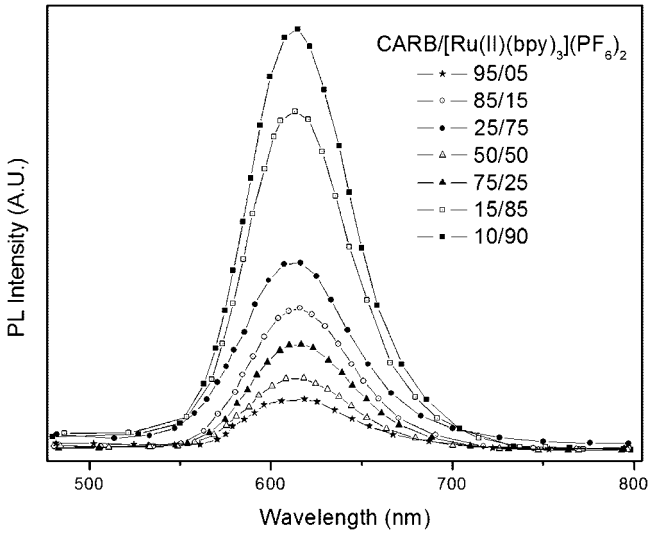

Figure 12. CARB/[Ru(II)(bpy)$_3$](PF$_6$)$_2$: 95/05 = ★, 85/15 = △, 75/25 = ▲, 50/50 = ○, 25/75 = ●, 15/85 = □, 10/90 = ■.

the broadness of the spectrum peaks. The ^{1}H NMR peak at 8.4−8.9 ppm, attributed to six of the bpy aromatic protons of the [Ru(vbpy)(bpy)$_2$]$^{2+}$ unit, and the broad peak from 5.6−7.3 ppm, attributed to six aromatic protons of the carbazole unit, were used for this estimation (Figure 4).

In an attempt to calculate the homopolymers' **P1** and **P2** molecular characteristics (M_n, M_w, PDI), we tried to perform GPC measurements with UV detection at 254 nm. This was unsuccessful, which is justified according to the literature,[15,16,28] since there are strong interactions of the ruthenium complexes with the polystyrene stationary phase of GPC columns. However, there are examples of successful GPC characterization of metal-containing polymers with comparatively low metal loading.[6,21,24,36] In our case, the high metal complex loadings of most of our polymers did not allow their characterization using GPC. Despite that, to prove once again the polymeric nature of these complexes, viscometric characterization was applied.[10,11,35] These measurements were performed for **P1**, **P2**, and **d** in DMF at 30 °C, and the results are summarized in Table 1. In addition, the inset in Scheme 3 shows the viscosity values obtained for polymers **P1d**, **P2a**−**c**, and monomer **d** for different concentrations; an increase in the reduced viscosity values is evident as the solution concentration decreases. Such a behavior can be explained in terms of the polyelectrolyte nature of the polymers due to the presence of Ru(II) and the PF_6^- counterions. Comparison of the viscosity values with those of the vinylic monomer **d**, as well as the relation of the viscosity value of polymer **P1d** with the M_n value obtained by ^{1}H NMR, fully supports the formation of polymeric hybrid materials in both the cases of **P1** and **P2**.

On the other hand, the copolymers of ruthenium complexes with oxadiazole units (**P3**) could be successfully characterized with GPC, but only for those having low metal loadings (less interaction with the polystyrene columns used). It was observed that in the cases of higher oxadiazole loadings (feed composition ratios of 95/05, 90/10, and 85/15) the copolymers were soluble in $CHCl_3$ and their GPC characterization was possible, as shown in Table 2. A representative GPC trace of **P3iii** copolymer is provided in the Supporting Information (Figure S2). Similarly, for the **P4** copolymers, GPC characterization was successful for high carbazole loadings (feed composition ratios of 95/05, 85/15, and 75/25), as shown in Table 3. A representative GPC trace of **P4iii** copolymer is provided in the Supporting Information (Figure S3) as well.

Optical Characterization. The [Ru(vbpy)(bpy)$_2$](PF$_6$)$_2$ unit (**d**), homopolymers **P1** and **P2**, and copolymers **P3** and **P4** were thoroughly characterized with respect to their optical properties in dilute DMF solutions (10^{-5}−10^{-6} M), via UV−vis and PL spectroscopies. In all cases the characteristic absorption and emission bands of the [Ru^{II}(bpy)$_3$]$^{2+}$ complexes were observed. On the other hand, for copolymers **P3** and **P4**, bands due to the synergistic effect of both the monomer **d** and OXD or CARB coexisting moieties could be detected, with varying intensities depending on the ratios of the comonomers. All homopolymers and copolymers present intense red light emissions.

Concerning the monomer **d** and the polymers **P1** and **P2**, UV−vis spectroscopy revealed identical spectra, exhibiting an absorption peak at around λ = 292 nm and a "shoulder" at λ = 320 nm, attributed to $\pi-\pi^*$ LC (ligand-centered) transitions of 2,2′-bipyridine, and an absorption maximum at λ = 458 nm, which is characteristic of the d−π^* MLCT (metal to ligand charge transfer) of the [Ru(vbpy)(bpy)$_2$](PF$_6$)$_2$ complexes (Figure 5). In the case of **P2**, where the anthracene unit is used as the initiator, one should expect an additional absorption peak at λ = 414 nm attributed to the anthracene unit, as shown in Figure 5, but particularly this peak is overlapped by the ruthenium complex absorption at 458 nm, since the concentration of the anthracene initiator in **P2** is very low.

Photoluminescence investigation of monomer **d** and polymers **P1** and **P2** after excitation at λ = 290 nm and λ = 320 nm revealed identical emission peaks located at around λ = 380 nm and λ = 615 nm attributed to the [Ru(vbpy)(bpy)$_2$](PF$_6$)$_2$ complex. Depending on the excitation wavelength, varying emission intensities were observed as

shown in Figure 6. Additionally, in the case of **P2**, due to the overlapping of the absorption band of monomer **d** and the anthracene moiety, after being excited either at $\lambda = 414$ nm (where the absorption maxima of the anthracene initiator is located) or at $\lambda = 458$ nm (attributed to monomer **d**), emissions at $\lambda = 520$ nm and $\lambda = 615$ nm were observed, proving the incorporation of the anthracene group along the polymeric backbone (Figure 6).

The UV−vis optical characterization of copolymers **P3** revealed similarities with those of polymers **P1** and **P2**. As shown in Figure 7, the d−π* MLCT absorption band of the $[Ru(vbpy)(bpy)_2](PF_6)_2$ unit is evident at $\lambda = 458$ nm. Moreover, **P3** copolymers exhibit a peak of higher intensity, with maxima either at $\lambda = 296$ nm (absorption maxima of the oxadiazole unit) or at $\lambda = 292$ nm (absorption of bpy ligands), plus a shoulder at around $\lambda = 320$ nm attributed to the $\pi-\pi$* LC transition of 2,2′-bipyridines, depending on the molar ratio of the copolymer. In that order, the absorption maxima observed for **P3i**−**vii** vary from 296 to 292 nm, whereas the shoulder at $\lambda = 320$ nm is observed only in cases of high metal loadings. Furthermore, it should be outlined that the intensity of the MLCT absorption band at 458 nm increases by increasing the ratio of the metal complex to the copolymer, whereas the absorption band at ∼294 nm remains relatively constant.

Photoluminescence spectra of copolymers **P3** were obtained after excitation at $\lambda = 290$ nm and $\lambda = 458$ nm with emission maxima at $\lambda = 382$ nm and $\lambda = 615$ nm (Figures 8 and 9). The first peak is attributed to the $\pi-\pi$* LC absorption band of both 2,2′-bipyridine and the oxadiazole unit, while the latter is characteristic only of the d−π* MLCT absorption band of the $[Ru(vbpy)(bpy)_2](PF_6)_2$ unit.

Concerning copolymers **P4**, their optical properties resemble those of **P3**. In the UV−vis spectra of copolymers **P4i**−**vii**, one can observe absorption peaks at $\lambda = 458$ nm characteristic of the d−π* MLCT absorption band of the $[Ru(vbpy)(bpy)_2](PF_6)_2$ unit as shown in Figure 10. Moreover, **P4** copolymers exhibit a peak of higher intensity, with a maximum located at $\lambda = 292$ nm and a shoulder at around $\lambda = 320$ nm, originating from the $\pi-\pi$* LC transition of 2,2′-bipyridine, as well as the carbazole units. Furthermore, it should be pointed out that the absorption intensity of the MLCT band increases compared to that at ∼292 nm, similarly to that of **P3**, by increasing the ratio of the metal complex to the copolymer.

Photoluminescence spectra of **P4** were obtained after excitation at $\lambda = 290$ nm (Figure S4, Supporting Information), $\lambda = 340$ nm (Figure 11), and $\lambda = 458$ nm (Figure 12). Emission peaks were observed at $\lambda = 382$ nm and $\lambda = 615$ nm. The first peak is attributed to the $\pi-\pi$* LC absorption band of 2,2′-bipyridine and to the carbazole unit, while the latter is characteristic of the d−π* MLCT absorption band of the $[Ru(vbpy)(bpy)_2](PF_6)_2$ unit. All copolymers **P4i**−**vii** exhibit similar spectral characteristics after excitation at the absorption maxima of the carbazole and the bipyridine unit at ∼290 nm. The emission wavelength range consists of bands at $\lambda = 380$ nm and $\lambda = 615$ nm. If excitation takes place at $\lambda = 340$ nm, where the carbazole moiety absorbs, the same emission bands appear (Figure 11). When the excitation wavelength is 458 nm, only emission peaks at $\lambda = 615$ nm are observed (Figure 12). All of the above optical data ensure the incorporation of the $[Ru(vbpy)(bpy)_2](PF_6)_2$ unit into the polymeric chains and the ability of these types of polymers and copolymers to incorporate the optical properties of the metallic complex.

Conclusions

The newly developed vinylbipyridine monomer **c** used in this work was synthesized from bromopyridine derivatives, taking advantage of the combination of Stille and Suzuki palladium-catalyzed coupling reactions. Complexation of this monomer with ruthenium ions resulted in the high-yield preparation of the $[Ru(vbpy)(bpy)_2](PF_6)_2$ complex (**d**). This vinylic complex was successfully employed in atom transfer radical polymerization, demonstrating for the first time the ability of such complexes to be polymerized via ATRP. Moreover, it was copolymerized via FRP with oxadiazole and carbazole monomers, producing copolymers with electron/hole transporting architectures, respectively. All polymers and copolymers were soluble in common organic solvents, despite their high metal loadings. A complete characterization via ^{1}H NMR, GPC, and viscosity measurements was performed. On the basis of the "architecture" of these polymers and copolymers, and their optical characteristics (UV−vis and PL), applications in optoelectronic devices seem quite feasible. The key advantage of this work, besides the high-yield synthesis of the new vinyl monomer **d**, is its direct ATR homopolymerization, using various functional initiators. These homopolymers bearing $[Ru^{II}(bpy)_3]^{2+}$ complexes on every single repeating unit were easily soluble in common organic solvents, allowing their thorough characterization with respect to their structural and optical characteristics. Moreover, the combination of the optical characteristics of the metal complex with the polymers' properties and more importantly with the electron or hole transporting characteristics of the comonomers employed is expected to further contribute to the balanced charge mobility of these materials.

Acknowledgment. Financial support for this project from the Greek Ministry of Development under Research Grant PENED 03ED118 "Organic Solar Cells" is gratefully acknowledged. This research project (PENED) is cofinanced by the EU European Social Fund (75%) and the Greek Ministry of Development, GSRT (25%).

Supporting Information Available: A representative ^{1}H NMR spectrum of the ATRP kinetic study of **P1e** along with GPC traces of **P3iii** and **P4iii** copolymers and the PL spectrum of copolymers **P4** after excitation at 290 nm. This material is available free of charge via the Internet at http://pubs.acs.org.

CM800911Y